

Matthias Schaufelberger\*, Reinald Kühle, Frederic Weichel, Andreas Wachter, Niclas Hagen, Friedemann Ringwald, Urs Eisenmann, Christian Freudsperger and Werner Nahm

# Laplace-Beltrami Refined Shape Regression Applied to Neck Reconstruction for Craniosynostosis Patients

Combining posterior shape models with a Laplace-Beltrami based approach for shape reconstruction

**Abstract:** This contribution is part of a project concerning the creation of an artificial dataset comprising 3D head scans of craniosynostosis patients for a deep-learning-based classification. To conform to real data, both head and neck are required in the 3D scans. However, during patient recording, the neck is often covered by medical staff. Simply pasting an arbitrary neck leaves large gaps in the 3D mesh. We therefore use a publicly available statistical shape model (SSM) for neck reconstruction. However, most SSMs of the head are constructed using healthy subjects, so the full head reconstruction loses the craniosynostosis-specific head shape. We propose a method to recover the neck while keeping the pathological head shape intact. We propose a Laplace-Beltrami-based refinement step to deform the posterior mean shape of the full head model towards the pathological head. The artificial neck is created using the publicly available Liverpool-York-Model. We apply our method to construct artificial necks for head scans of 50 scaphocephaly patients. Our method reduces mean vertex correspondence error by approximately 1.3 mm compared to the ordinary posterior mean shape, preserves the pathological head shape, and creates a continuous transition between neck and head. The presented method showed good results for reconstructing a plausible neck to craniosynostosis patients. Easily generalized it might also be applicable to other pathological shapes.

**Keywords:** Statistical Shape Modeling, Craniosynostosis, Scaphocephaly, Laplace-Beltrami, Shape Reconstruction, Posterior Shape Model

<https://doi.org/10.1515/cdbme-2021-2049>

## 1 Introduction

### 1.1 Clinical Motivation

Craniosynostosis manifests in characteristic head deformities and can lead to elevated intracranial pressure resulting in limited brain growth. Early diagnosis is crucial for surgical planning and clinical treatment. Although radiation-free classification approaches by means of machine learning have been proposed [1], computed tomography (CT) remains the gold standard for classification. It has been shown that head deformities of craniosynostosis can be captured using 3D photogrammetric scans [2]. Robust classifiers using 3D surface scans or 2D image data derived from surface scans could eliminate the need of CT thus avoiding ionizing radiation for infants. However, 3D surface scans of craniosynostosis patients are sparse, so we plan to construct a large dataset craniosynostosis patients using a Statistical Shape Model (SSM). Our long-term goal is to create 3D and 2D image data for deep-learning-based classifiers. The synthetic image data needs to contain both the characteristic head deformity of craniosynostosis as well as a full head including face and neck to conform to real data.

### 1.2 Shape Reconstruction

Posterior shape modeling is one of the most suitable methods for shape reconstruction. It allows incorporating a-priori

\*Corresponding author: **Matthias Schaufelberger:** Karlsruhe Institute of Technology, Institute of Biomedical Engineering, Karlsruhe, publications@ibt.kit.edu

**Reinald Kühle, Frederic Weichel, Christian Freudsperger:** Clinic of Oral and Maxillofacial Surgery, Heidelberg University Hospital, Heidelberg, Germany

**Niclas Hagen, Friedemann Ringwald, Urs Eisenmann:** Institute of Medical Informatics, Heidelberg University Hospital, Heidelberg, Germany

**Andreas Wachter, Werner Nahm:** Karlsruhe Institute of Technology, Institute of Biomedical Engineering, Karlsruhe, Germany

knowledge about the shape, modeled as a probabilistic function based on real data [3]. Consequently, the shape reconstruction is restricted to shape attributes provided by the shape model, i.e., to the training data which was used to construct the SSM. If an SSM is constructed from subject with normal head shape, the posterior mean shape will also be a normally-shaped head. To the best of our knowledge, there are no publicly available head models constructed from craniosynostosis patients to date, so we have to use a publicly available SSM of the healthy head with the necessity to recover the pathological head shape. In this contribution, we propose a Laplace-Beltrami-based deformation step to obtain a full head with neck and the craniosynostosis-specific head deformity. We propose a two-step-approach using a posterior shape model [3] and a modified version of a Laplace-Beltrami-based As-Rigid-As-Possible morphing [4].

## 2 Methods

### 2.1 Dataset and Preprocessing

For this study, we used 3D stereo photographs of scaphocephaly patients, acquired in the Department of Oral and Maxillofacial Surgery of the Heidelberg University Hospital, Heidelberg, Germany in the years 2011 to 2020. All scans were recorded using a VECTRA-360-nine-pod system (Canfield Science, Fairfield, NJ, USA) and annotated with 10 cephalometric landmarks by trained medical staff. We selected 50 patients diagnosed with scaphocephaly. The mean age of the selected patients is  $0.55 \pm 0.29$  years.

As the children were held by medical staff during recording, neck and upper torso are either covered by the children's clothes or the hands of medical staff. We therefore aim for reconstructing an artificial, but realistic-looking neck using a SSM. We use the Liverpool York Child Head Model (LYCHM) constructed from children between 2 and 15 years ( $8.9 \pm 3.3$  years) [4] with the idea to reconstruct a plausible neck for all our patients.

For correspondence establishment, we extracted the craniofacial part of the LYCHM and performed the LB regularized projection of [4] using the mean shape of the LYCHM. Note that the template shape is arbitrary, if it shares the same point identifiers as the SSM and has the same triangular mesh structure we use for shape reconstruction later. The full observation (cranium and neck) has  $p = 11510$  points, the partial observation (cranium only) has  $p = 10620$  points.

### 2.2 Shape regression with Laplace Beltrami regularized refinement

When dealing with observations and SSMs general, we need to remove non-shape related components (rotation, translation, and scaling) from the  $p$  points of any unaligned observation  $\mathbf{X}_u \in \mathbb{R}^{p \times 3}$  first. This alignment step can be performed using Procrustes Analysis applied to vertex-to-vertex correspondences to compute rotation matrix  $\mathbf{R} \in \mathbb{R}^{3 \times 3}$ , translation vector  $\mathbf{t} \in \mathbb{R}^3$ , and isotropic scaling  $s$  between  $\mathbf{X}_u$  and the mean shape  $\mathbf{M} \in \mathbb{R}^{p \times 3}$  of the SSM. We can therefore obtain the aligned observation  $\mathbf{X}$  using

$$\mathbf{X} = s \cdot \mathbf{R} \cdot \mathbf{X}_u + \mathbf{t}^T. \quad (1)$$

To align partial observations with  $q$  points with  $q < p$ , we simply select the  $q$  vertices from the mean shape  $\mathbf{M}$  and use eq. 1 in an analogous manner.

Regarding the shape model notation, we will mainly rely on [3]. We convert the block matrix  $\mathbf{X}$  into column vector  $\mathbf{x} \in \mathbb{R}^{3p}$  (and analogous  $\mathbf{M}$  into  $\boldsymbol{\mu}$ ) using

$$\mathbf{x} = \text{col}(\mathbf{X}) = \begin{pmatrix} x_1 \\ y_1 \\ z_1 \\ x_2 \\ \vdots \\ z_n \end{pmatrix}, \boldsymbol{\mu} = \text{col}(\mathbf{M}). \quad (2)$$

The SSM consists of mean shape  $\boldsymbol{\mu} \in \mathbb{R}^{3p}$  and sample covariance matrix  $\boldsymbol{\Sigma} \in \mathbb{R}^{3p \times 3p}$ .  $\boldsymbol{\Sigma}$  can be decomposed using eigenvalue decomposition  $\boldsymbol{\Sigma} = \mathbf{U}\mathbf{D}^2\mathbf{U}^T \in \mathbb{R}^{3p \times 3p}$ . It can be reduced to its first  $n$  eigenvalues in diagonal form  $\mathbf{D} \in \mathbb{R}^{n \times n}$  and the first  $n$  principal components  $\mathbf{U} \in \mathbb{R}^{3p \times n}$ . With the principal component matrix  $\mathbf{Q} = \mathbf{U}\mathbf{D} \in \mathbb{R}^{3p \times n}$ , we can represent a shape of the SSM as a combination of  $\boldsymbol{\mu}$ ,  $\mathbf{Q}$ , and coefficient vector  $\boldsymbol{\alpha} \in \mathbb{R}^n$  using

$$\mathbf{x} = \boldsymbol{\mu} + \mathbf{Q} \cdot \boldsymbol{\alpha}. \quad (3)$$

For a given partial observation of  $q$  points  $\mathbf{x}_g = \text{col}(\mathbf{X}_g) \in \mathbb{R}^{3q}$ , we usually cannot find any  $\boldsymbol{\alpha}$  according to eq. 3 to match the observation perfectly. We rather match it in terms of an observation noise  $\boldsymbol{\epsilon} \in \mathbb{R}^{3q}$ . By selecting the corresponding rows and columns in  $\mathbf{Q}$  for the  $q$  points we obtain  $\mathbf{Q}_g \in \mathbb{R}^{3q \times n}$  and can model  $\mathbf{x}_g$  as

$$\mathbf{x}_g = \boldsymbol{\mu}_g + \mathbf{Q}_g \cdot \boldsymbol{\alpha} + \boldsymbol{\epsilon}. \quad (4)$$

According to [3], the posterior mean shape (PMS)  $\boldsymbol{\mu}_c \in \mathbb{R}^{3p}$  of the conditional distribution can be calculated using

$$\boldsymbol{\mu}_c = \boldsymbol{\mu} + \mathbf{Q}(\mathbf{Q}_g^T \mathbf{Q}_g + \sigma^2 \mathbf{I}_n)^{-1} \mathbf{Q}_g^T (\mathbf{x}_g - \boldsymbol{\mu}_g). \quad (5)$$

$\sigma$  models the variance of the observation. For  $\sigma \rightarrow 0$ , we demand that the SSM match the observation accurately, which usually leads to an over-emphasis of the noisy components of the SSM. Increasing  $\sigma$  allows the SSM more flexibility for fitting the observation.

The PMS is a representation of the full shape created from the SSM. Features not present in the training data are not yet represented in the reconstruction. If mapped the partial observation directly onto the reconstructed shape, we would create a gap between the partial observation and the reconstruction.

By converting  $\boldsymbol{\mu}_c = \text{col}(\mathbf{M}_c)$  and  $\mathbf{x}_g = \text{col}(\mathbf{X}_g)$  back into their respective matrix form (analogous to eq. 2), we can proceed with the LB regularized refinement. We use the LB regularized projection [4] to deform the reconstruction to match the partial observation.  $\mathbf{L}_c \in \mathbb{R}^{p \times p}$  denotes the LB Operator of the PMS  $\mathbf{M}_c \in \mathbb{R}^{p \times 3}$ . We solve the system of linear equations for the refined points  $\mathbf{X}_r \in \mathbb{R}^{p \times 3}$ , which is given by

$$\begin{pmatrix} \lambda \mathbf{L}_c \\ \mathbf{S}_c \end{pmatrix} \mathbf{X}_r = \begin{pmatrix} \lambda \mathbf{L}_c \cdot \mathbf{M}_c \\ \mathbf{I}_g \cdot \mathbf{X}_g \end{pmatrix}. \quad (6)$$

$\mathbf{I}_g \in \mathbb{R}^{q \times q}$  denotes the identity and  $\mathbf{S}_c \in \mathbb{R}^{q \times p}$  denotes a Boolean selection matrix. For each of the observed points  $q$  of  $\mathbf{X}_g$  we selected the corresponding vertex from the  $p$  vertices of  $\mathbf{X}_r$  which we are solving for. This equation balances retaining the morphology of the PMS  $\mathbf{M}_c$  and mapping the partial observation  $\mathbf{X}_g$ . By changing the regularization parameter  $\lambda$ , we can put more weight to either the correspondences of the morphology or the PMS. It can therefore be described as the "stiffness" of the transformation. For  $\lambda \rightarrow \infty$ , the result is the rigidly transformed  $\mathbf{M}_c$ , for  $\lambda \rightarrow 0$ , we map the observation almost directly and create an irregular mesh.

For the two parameters  $\sigma$  and  $\lambda$  introduced in eq. 5 and eq. 6, we choose  $\sigma = 1$  and  $\lambda = 1$ .

### 2.3 Evaluation of reconstruction methods

We quantitatively evaluated our proposed LB refined morphing approach on 50 scaphocephaly patients using correspondence errors on the head between the reconstruction and the observation. With respect to the neck, a smooth transition from the head to the artificial neck is desirable. We assessed the transition by computing the gap length reduction between the boundary sets of head and neck, compared with the distance when simply mapping the partial observation onto the PSM. Qualitatively, we evaluated the fit in terms of regularity of the mesh on the transition of head and neck.

## 3 Results

Although evaluated on all 50 subjects, for qualitative metrics, we exemplify our results on one subject (S1). Quantitative results were evaluated on all 50 subjects. Figure 1 shows the reconstruction for the PMS and our proposed LB refined approach. While the PSM shows large regions with absolute correspondence errors higher than 2 mm on the face and the cranium, the LB refined approach shows errors between  $\pm 1$  mm. Note that we restricted the color scale to  $\pm 2$  mm for the sake of comparability, although the maximum absolute correspondence error of the PSM is 9.7 mm. The PMS resembles a shape without scaphocephaly while the proposed LB refined approach shows good accordance with the elongated head of a scaphocephaly patient.

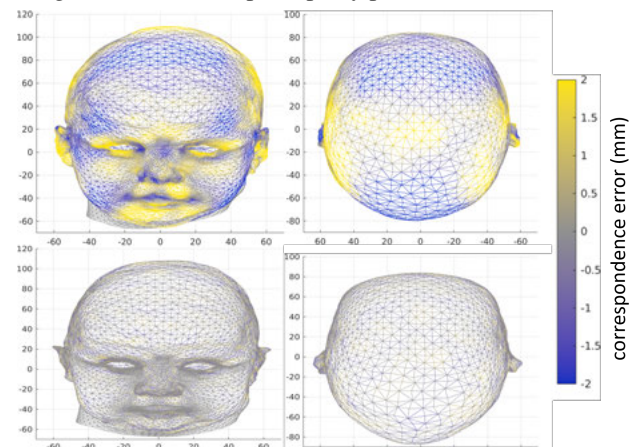


**Figure 1:** Correspondence errors of reconstructions exemplified on S1. Top row: PMS, bottom row: LB refined. Left: Front view, right: top view. Color scale limited to  $\pm 2$  mm.

Figure 2 shows the region where the left neck transitions into the left head parts. As opposed to a direct mapping, neither the PMS, nor the proposed LB refined approach show a gap.

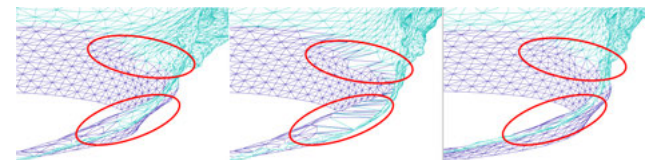


**Figure 2:** Boundary of head and neck exemplified on S1. From left to right: PMS, mapped, and LB refined.

Figure 3 shows the correspondence errors for the PMS and the LB refined reconstructions for all 50 subjects. The PMS based reconstruction consistently yield higher errors than the proposed LB refined approach. While median correspondence errors for PMSs are approximately 1.9 mm, median

correspondence errors for the LB refined reconstructions are around 0.6 mm.

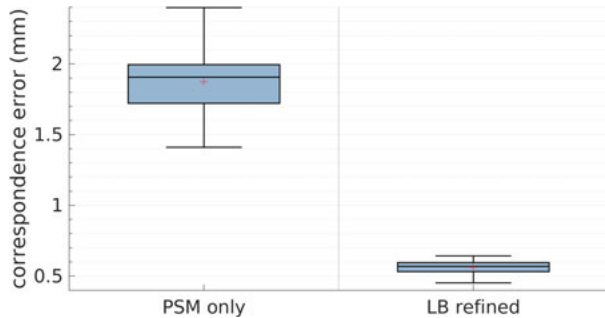


**Figure 3:** Mean correspondence error on the head for all 50 subjects.

Figure 4 shows that both PMS and the proposed LB refined approach reduce the mean gap distance for all 50 subjects using both methods. The mean and median reduction is around 0.3 mm. This corresponds to a reduction of more than 10% as the mean of the mean edge length of the PMS was 2.62 mm.

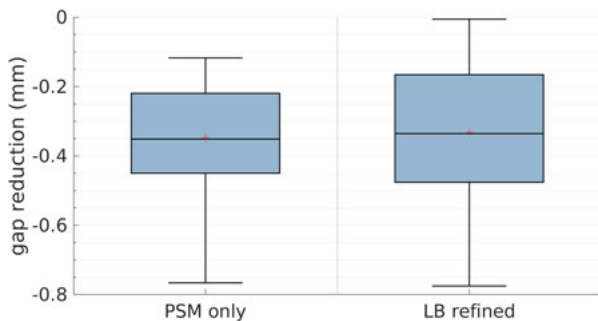


**Figure 4:** Mean gap reduction on the boundary of head and neck for all 50 subjects.

## 4 Discussion

We proposed a refined shape reconstruction method using an LB-based refinement of a posterior shape model. The proposed LB refined reconstruction method reduces reconstruction errors compared with the PMS while also allowing a smooth transition from the original observation to the reconstructed part. Shape features not present in the PMS could be re-established using the proposed LB refined reconstruction. This includes shape differences and the subjects' faces most likely introduced by age and ones introduced by head shape. We provided a general description of our method which makes it applicable to a variety of shapes.

Our study has several limitations. The first limitation concerns the limited variability of both dataset and application

that we provided. Given the nature of craniosynostosis, we only tested our approach on 50 patients younger than 1.5 years. We also applied our method only to neck reconstruction. When generalizing, the results should be interpreted carefully. Secondly, we used a large, homogeneous, and connected region as partial observation which might explain why the LB refined approach was able to fit the observation to the PMS well. Furthermore, the partial observations contain little noise. As the LB refined fit does not consider observation noise, it might be very sensitive to noisy observations or wrong correspondences, especially for isolated and scattered observation points.

## 5 Conclusion

We showed that our proposed LB refined shape reconstruction method shows good results for reconstructing a plausible neck for 50 scaphocephaly patients. As opposed to ordinary posterior shape modeling, our method can be applied even if the SSM has significant differences in its training data population. Our approach should be tested in terms of robustness and its suitability for other shapes. Further applications of our method include the creation of synthetic dataset for machine learning approaches which are dependent on a conform dataset.

### Author Statement

Research funding: This study is part of the HEiKA research project HEiKA\_19-17. Conflict of interest: Authors state no conflict of interest.

## References

- [1] G. de Jong, E. Bijlsma, J. Meulstee, M. Wennen, E. van Lindert, T. Maal, R. Aquarius, and H. Delye, "Combining deep learning with 3D stereophotogrammetry for craniosynostosis diagnosis.," *Sci Rep*, vol. 10, no. 1, p. 15346, Sep. 2020.
- [2] J. W. Meulstee, L. M. Verhamme, W. A. Borstlap, F. Van der Heijden, G. A. De Jong, T. Xi, S. J. Bergé, H. Delye, and T. J. J. Maal, "A new method for three-dimensional evaluation of the cranial shape and the automatic identification of craniosynostosis using 3D stereophotogrammetry.," *Int J Oral Maxillofac Surg*, vol. 46, no. 7, pp. 819–826, Jul. 2017.
- [3] T. Albrecht, M. Lüthi, T. Gerig, and T. Vetter, "Posterior shape models.," *Med Image Anal*, vol. 17, no. 8, pp. 959–73, Dec. 2013.
- [4] H. Dai, N. Pears, W. Smith, and C. Duncan, "A 3D Morphable Model of Craniofacial Shape and Texture Variation," in *2017 IEEE International Conference on Computer Vision*, 2017, pp. 3104–3112.